Available online at www.sciencedirect.com

ScienceDirect

IFAC Papers Online CONFERENCE PAPER ARCHIVE

IFAC PapersOnLine 50-1 (2017) 7592–7597

Iterative Learning Control of a Pneumatically Actuated Lung Tumour Mimic Model

Alexander Wache * **Harald Aschemann** * **Robert Prabel** * **Jens Kurth** ** **Bernd J. Krause** ** **Stefan Zorn** ***

* *Chair of Mechatronics, University of Rostock, D-18059 Rostock, Germany, (e-mail:{Alexander.Wache, Harald.Aschemann, Robert.Prabel}@uni-rostock.de).*

** *Department of Nuclear Medicine, University Medical Center of Rostock, D-18057 Rostock, Germany, (e-mail: {Jens.Kurth, Bernd.Krause}@uni-rostock.de).*

*** *Chair of Mechanical Engineering Design/CAD, University of Rostock, D-18059 Rostock, Germany, (e-mail: Stefan.Zorn@uni-rostock.de).*

Abstract: In this paper, a model-based tracking control is proposed for a mechanism dedicated to accurately reproduce the breathing-induced motion of a human lung tumour. A lung tumour mimic model should perform the same smooth motion as a real one in a human body during inhalation and exhalation. In former work, a 3-dimensional mechanism equipped with three pneumatically driven axes has been developed and built up for this purpose. The discrete-time control structure consists of cascaded control loops: In the fast inner loops, the chambers pressures of the pneumatic cylinders are controlled, whereas the outer loops are related to the position control of the cylinders. Furthermore, iterative learning controllers are employed to compensate model uncertainties and lumped disturbance forces. The proposed overall control structure has been implemented and successfully validated on the innovative test rig.

Keywords: Tumour mimic model, cascaded control, iterative learning control, pneumatics, friction compensation.

1. INTRODUCTION

In the framework of medical research, suitable mechanisms with mimic models are often required. They are either used to validate experimental set ups in radiology or computed tomography (CT) imaging. In many cases, these specially designed mechanisms or small-scale robots are actuated pneumatically. In comparison to regular electro-mechanical or hydraulic solutions, pneumatic drives benefit from low investment costs, a clean working medium and steady-state actuation without thermal problems. From a control point of view, however, a characteristic drawback of pneumatically actuated systems is given by the air compressibility, which has to be taken into account properly at control design. In addition, the nonlinear kinematics of the mechanical mechanism or the small-scale robot and nonlinear friction have to be considered. Especially the friction in the pneumatic actuators ends up becoming a significant barrier to precise motion.

In Fischer et al. (2008), a pneumatically actuated robotic assistant is presented, used for magnetic resonance imaging. The robot is capable of placing a needle to the patient with high accuracy. Another pneumatically driven robot is described in Kapoor et al. (2009). Here, the robot has to fulfil medical tasks with a hands-on cooperative control. A backstepping control approach is presented for a pneumatic needle-guiding robot in Franco et al. (2015). A pneumatic needle driver is also discussed in Comber et al. (2016). The applied hybrid control concept meets given performance criteria for positions as well as speeds in both translational and rotary directions.

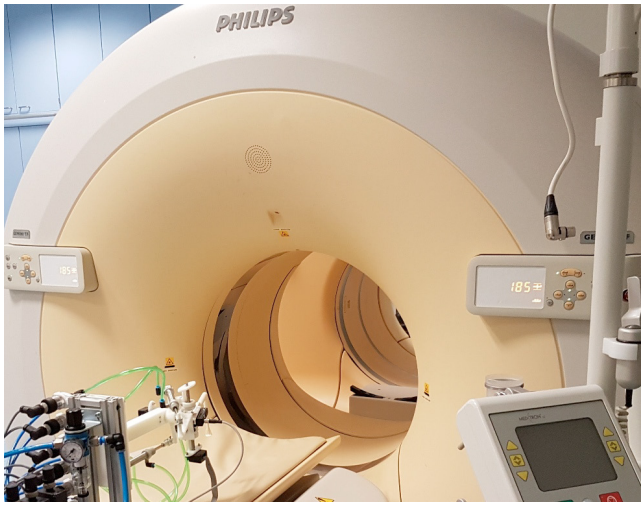

Fig. 1. Test rig in front of a Philips PET/CT scanner at the University Medical Center of Rostock.

A possible application is depicted in Fig. 1. Here, the tumour mimic robot is used inside a PET/CT scanner from Philips to simulate the breathing-induced motion of a human lung tumour. A clinically validated mathematical model for such a motion is presented in Seppenwoolde et al. (2002) and Prabel et al. (2016).

This paper is structured as follows: First, a control-oriented model of the mechatronic system including identified valve

2405-8963 © 2017, IFAC (International Federation of Automatic Control) Hosting by Elsevier Ltd. All rights reserved.
Peer review under responsibility of International Federation of Automatic Control.
10.1016/j.ifacol.2017.08.1003

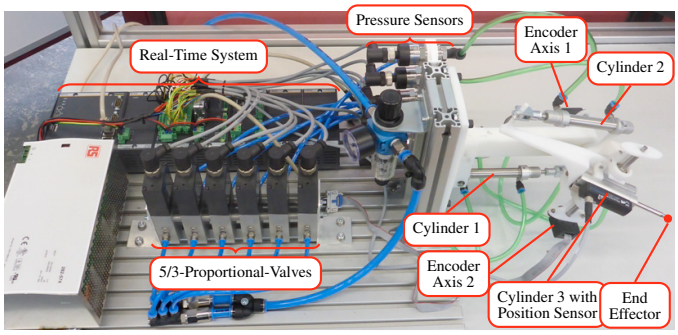

Fig. 2. Test rig with a mechanism allowing for a 3-dimensional motion of a lung tumour mimic model.

characteristics is derived in Sec. 2. Second, the cascaded nonlinear control design using flatness techniques is presented, which consists of a fast inner loop for the cylinder pressures and an outer loop for the cylinder positions. Third, an iterative learning controller is designed for each axis to learn the repeating tracking error. This controller modifies the desired trajectory in such a way that the resulting tracking error is reduced. Moreover, the implementation of the overall control structure on a dedicated test rig is discussed. Finally, the paper finishes with an experimental validation and a short summary.

2. MODELING OF THE TEST RIG

2.1 Test Rig Design

The innovative test rig at the Chair of Mechatronics, University of Rostock, is shown in Fig. 2. The white structure elements have been produced with a 3D-printer, which allows for a lightweight design with optimized geometry even for a prototype. The end effector position is determined by three pneumatic cylinders, where each chamber of the pneumatic cylinders is equipped with an individual pressure sensor as well as a proportional valve. An accurate measurement of the joint angles is achieved with two incremental encoders, whereas the displacement of the third cylinder is measured by a magnetic position sensor.

The mechatronic system can be structured in kinematical, mechanical, and pneumatic subsystems. The kinematics represents the nonlinear transformation between the end effector coordinates and the individual cylinder positions. The mechanical subsystems describe the cylinder motions, whereas the pneumatic subsystems cover the pressure dynamics in the chambers of the pneumatic cylinders as well as the air mass flows through the proportional valves.

2.2 Kinematical Subsystem

In this section, the mathematical relations between the end effector position, the generalised coordinates and the positions of the three pneumatic actors are established. The positions of the cylinders $\underline{x}_C$ are determined by the generalised coordinates $\underline{\varphi}$ of the robot, which comprise two rotatory and one translatory degree of freedom. The generalised coordinates $\underline{\varphi}$ can be calculated from the vector of the cylinder positions $\underline{x}_C$ by an invertible nonlinear transformation as follows

$$\underline{\varphi} = \underline{T}_1(\underline{x}_C). \tag{1}$$

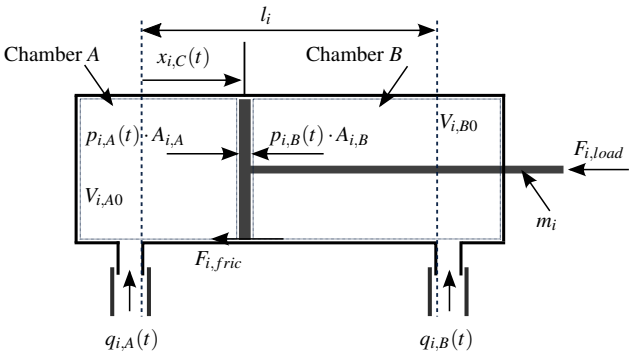

Fig. 3. Structure of the pneumatic cylinder.

Given the vector $\underline{\varphi}$ of the generalised coordinates, the position of the end effector $\underline{r}_{03}$ becomes

$$\underline{r}_{03} = \underline{T}_2(\underline{\varphi}). \tag{2}$$

The transformations $\underline{T}_1$ and $\underline{T}_2$ result from the geometry of the robot. By inverting those relations and substituting (2) in (1), the envisaged relation between the end effector and the cylinder positions can be stated as

$$\underline{x}_C = \underline{T}_1^{-1}\left(\underline{T}_2^{-1}(\underline{r}_{03})\right) . \tag{3}$$

A more in-depth analysis of the robot kinematics can be found in Prabel et al. (2016).

2.3 Mechanical Subsystem of the Pneumatic Cylinders

As depicted in Fig. 3, the pressure-dependent forces $A_{i,A}\, p_{i,A}(t)$ and $A_{i,B}\, p_{i,B}(t)$ act on the piston of the cylinder i. The resulting force is denoted as $\Delta F_i(t)$ and serves as control input for the mechanical subsystems. $A_{i,A}$ and $A_{i,B}$ identify the surface areas of the piston. Nonlinear friction forces $F_{i,fric}$ and unknown load forces $F_{i,l}$ are combined in a lumped disturbance force $F_{i,U}$ to be estimated. Note that $F_{i,U}$ takes parameter uncertainty into account as well. Given the lightweight design of the mechanism and the relatively slow desired trajectory for the end effector, any inertia effects of the robot structure can be neglected in the modelling part. This corresponds to a purely kinematic description of the robot. In any case, friction forces as well as model uncertainties are addressed properly by the lumped disturbance forces $F_{i,U}$. Finally, a balance of momentum yields the equation of motion for each cylinder

$$\ddot{x}_{i,C}(t) = \frac{1}{m_i}[\Delta F_i(t) - F_{i,U}(t)], \tag{4}$$

with m_i as the reduced mass of all the moving components of each pneumatic cylinder.

2.4 Pneumatic Subsystem

The dynamics of the internal pressures, which is presented exemplary for chamber A, follows directly from a mass flow balance in combination with a polytropic change of thermodynamic state for the compressed air in the cylinder chamber. As the supply pressure p_S is at a value of approx. $p_S = 2$ bar, the ideal gas equation $p_{i,A}(t) = \rho(t) \cdot R_L \cdot T(t)$ represents an accurate description of the thermodynamic behaviour of the compressed air. Here, the density $\rho(t)$, the gas constant of air R_L and the thermodynamic temperature $T(t)$ are introduced. The thermodynamic process is modelled as a polytropic change of state according to $p_{i,A}(t)\rho^{-n}(t) = \text{const.}$, where $n = 1.2$ represents the identified polytropic exponent. The relationship